

ORIGINAL ARTICLE: RESEARCH

Vorinostat induced cellular stress disrupts the p38 mitogen activated protein kinase and extracellular signal regulated kinase pathways leading to apoptosis in Waldenström macroglobulinemia cells

JENNY Y. SUN¹, HSIUYI TSENG¹, LIAN XU¹, ZACHARY HUNTER¹,
BRYAN CICCARELLI¹, MARIATERESA FULCINITI¹, BANGMIN ZHU¹,
KAVEH MAGHSOUDI³, GUANG YANG^{1,2}, PING GONG¹, YANGSHENG ZHOU^{1,2},
XIA LIU¹, NIKHIL C. MUNSHI^{1,4}, CHRISTOPHER J. PATTERSON¹, &
STEVEN P. TREON^{1,2}

¹Bing Center for Waldenström's Macroglobulinemia, Dana-Farber Cancer Institute, Boston, MA, USA, ²Harvard Medical School, Boston, MA, USA, ³Harvard School of Public Health, Boston, MA, USA, and ⁴Boston VA Healthcare System, Boston, MA, USA

(Received 21 August 2010; revised 29 March 2011; accepted 30 March 2011)

Abstract

Histone deacetylases (HDACs) are aberrantly expressed, and inhibitors of HDACs induce apoptosis in lymphoplasmacytic cells (LPCs) in Waldenström macroglobulinemia (WM). The molecular profile by which these agents induce apoptosis in WM LPCs remains to be delineated. We examined the activity of the histone deacetylase inhibitor, vorinostat, and dissected its pro-apoptotic pathways in WM LPCs. Vorinostat induced apoptosis in WM cells through activating specific caspases at varying times. Inhibitors of apoptosis (IAPs) were down-regulated after vorinostat treatment. Cellular stress induced in vorinostat-treated WM cells was reflected by changes in the mitogen activated protein kinase (MAPK) pathways. Activated phospho-p38 MAPK was up-regulated at 12 h, while phospho-extracellular signal-regulated kinase (Erk) abruptly decreased at 24 h. Bortezomib did not augment vorinostat induced primary WM cell killing as reported in other B-cell disorders. These studies support that stress induced apoptosis in vorinostat-treated WM LPCs is mediated through disrupting the activity of the Erk and p38 MAPK pathways.

Keywords: Lymphoma and Hodgkin disease, lymphocytes, cell lines and animal models, chemotherapeutic approaches

Introduction

Waldenström macroglobulinemia (WM) is a low-grade lymphoproliferative disorder characterized by bone marrow infiltration of lymphoplasmacytic cells and the production of monoclonal immunoglobulin (IgM) protein [1,2]. Despite advances in treatment, WM remains incurable. As such, novel therapies based on WM molecular targets are needed.

Using gene expression profiling, we observed that the expression of histone deacetylases in primary WM CD19+ cells was different from that of healthy donor CD19+ cells [3]. Histone deacetylases

(HDACs) are involved in transcription regulation and signal transduction through the modification of histones and non-histone proteins [4]. The discovery of HDAC/co-repressor complexes was the basis for the rational design of HDCA inhibitors, which were shown to block leukemic cell maturation [5,6]. Further pharmacologic modification of HDAC inhibitors improved their potency to the micromolar range [6]. The HDAC inhibitors include benzamide derivatives, such as MS-275, and hydroxamic acid derivatives, such as vorinostat (suberoylanilide hydroxamic acid; SAHA) [7]. Vorinostat exhibits a wide

range of activity, including reactivation of leukemic cell differentiation, re-expression of tumor suppressor genes, induction of reactive oxygen species (ROS), modulation of nuclear factor- κ B (NF- κ B) pathways, disruption of heat shock protein (HSP) function, perturbation of Bcl-2 family members, and activation of extrinsic apoptotic pathways [8–12].

The initiation of apoptosis requires the activation of caspase cascades, which are regulated in part by members of the inhibitors of apoptosis (IAP) family. IAPs are evolutionarily conserved proteins among viruses, yeasts, nematodes, fish, flies, and mammals. In humans, eight members are currently described, including NAIP, cIAP1, cIAP2, XIAP, survivin, apollon, livin, and testicular specific-IAP (Ts-IAP) [13]. IAPs are known to prevent caspases from cleavage *in vitro*, and are able to delay the cell death response to apoptotic stimuli when overexpressed [14]. In IAP-deleted mice, NAIP, cIAP2, and XIAP promote the survival of neurons, cardiomyocytes, or macrophages in stress conditions, such as hypoxia, anoxia, and serum deprivation [15–17]. The presence of an internal ribosome entry site (IRES) element and an upstream open reading frame in a few IAPs allows continuous translation of these selective proteins only under stress conditions, while translation is shut off globally [18–20]. More recently, endoplasmic reticulum (ER) stress has been shown to induce the expression of IAPs [21]. In HDAC inhibitor treated cells, increased ROS, disrupted HSPs, and dysregulated transcription escalate ER stress, which could result in altered expression of IAPs as well as mitogen activated protein kinase (MAPK) pathways.

Three mammalian MAPKs have been well studied, including extracellular signal regulated kinase (Erk), c-jun NH₂-terminal kinase (JNK), and p38 MAPK. They are proline-directed protein kinases that relay intra- and extracellular stimuli on cellular proliferation, differentiation, and death. Growth factors and mitogenic stimuli usually activate Erk, while stress signals such as ultraviolet irradiation, osmotic stress, pro-inflammatory cytokines, and anti-cancer drugs activate JNK and p38 MAPK. Constitutive activation of the MAPK pathways drive the oncogenic transformation of fibroblast cells, and is often detected in human cancer cells harboring a variety of genetic mutations [22,23]. Andreeff's group has shown that inappropriate MAPK phosphorylation is an independent predictor of poor response to chemotherapy and shorter survival in patients with acute myeloid leukemia (AML) [24]. Lee *et al.* [25] have shown that phosphoacetylation of histone H3 occurs through activation of both Erk and p38 MAPK during early embryonic stem cell differentiation. Cancer cells share many properties of embryonic stem cells in that they can self-renew as well as proliferate

indefinitely [26]. It is conceivable that epigenetic modifications and the cellular stress response induced by HDAC inhibitors work in concert, leading to either differentiation or apoptosis of tumor cells.

Several of the HDAC specific inhibitors are being investigated clinically in other B-cell malignancies, alone and in combination therapy, including with the proteasome inhibitor bortezomib, where additive and potentially synergistic activity has been observed [27–31]. Bortezomib is active in both upfront as well as relapsed/refractory WM, producing response rates of 60–80%. As part of these efforts, we sought to elucidate the activity of the prototypic HDAC inhibitor, vorinostat, and to delineate its molecular mechanisms in WM as monotherapy and in combination therapy with bortezomib in BCWM.1 cells and primary WM tumor cells.

Materials and methods

Cells

The BCWM.1 cell line is derived from a patient with untreated WM [32]. Primary WM cells were obtained from the bone marrow of previously treated patients with WM, and sorted by CD19+ microbead selection (Miltenyi Biotec, Germany) with >90% purity as confirmed by flow cytometric analysis with human monoclonal CD20-phycoerythrin (PE) antibody (BD Bioscience, CA). Previous therapies for patients whose cells were used in this study included fludarabine/rituximab ($n=3$), cyclophosphamide based rituximab therapy ($n=4$), and bortezomib based therapy ($n=2$). Peripheral blood mononuclear cells (PBMCs) were obtained from healthy subjects after the removal of red blood cells with Human RBC lysis buffer (Boston BioProducts, MA). Cells were cultured at 37°C in RPMI 1640 containing 10% fetal bovine serum (Sigma-Aldrich Corp., MO), 2 mmol/L of L-glutamine, 100 units/mL of penicillin, and 100 µg/mL of streptomycin (Invitrogen, CA). Approval for these studies was obtained from the Dana-Farber Cancer Institute Review Board. Informed consent was obtained from all patients and healthy volunteers in accordance with the Declaration of Helsinki.

Reagents

Vorinostat with a purity of >97% was commercially obtained. A 10 mM stock solution of vorinostat was dissolved in dimethylsulfoxide (DMSO) and stored at –80°C; it was diluted in culture medium (0–50 µM) immediately before use. The maximum final concentration of DMSO (<0.1%) did not affect cell viability or induce cytotoxicity in all the cell lines and primary cells. Bortezomib was commercially

obtained. A 1 mg/mL stock solution of bortezomib was dissolved in phosphate buffered saline (PBS) and stored at -80°C ; the stock solution was diluted in culture medium (5–100 pg/mL) before use.

Apoptosis assay

Apoptosis was determined by flow cytometry using annexin V–fluorescein isothiocyanate (FITC) and propidium iodide (PI) staining. BCWM.1 cells (0.5×10^6 cells/well) were cultured in 24-well Falcon plates (BD Labwear, NJ) for 24 h with medium alone or with vorinostat (0–5 μM) in the presence or absence of sublethal doses of bortezomib (0–45 pg/mL). Cells were harvested and centrifuged for 4 min at 2000 rpm. Cells were subsequently re-suspended at 1×10^6 cells/mL in binding buffer (10 mmol/L HEPES buffer [4-(2-hydroxyethyl)-1-piperazineethanesulfonic acid], pH 7.4, 150 mmol/L NaCl, 5 mmol/L KCl, 1 mmol/L MgCl_2 , 1.8 mmol/L CaCl_2), and stained with annexin V–FITC and PI in the dark for 15 min. Cells were analyzed by flow cytometry.

Immunoblotting

BCWM.1 cells were lysed using protein lysis buffer (Cell Signaling Technology, MA), and reconstituted with 5 mmol/L of NaF, 2 mmol/L of Na_3VO_4 , 1 mmol/L of polymethylsulfonyle fluoride, 5 $\mu\text{g/mL}$ of leupeptine, and 5 $\mu\text{g/mL}$ of aprotinin. Whole cell lysates were subjected to sodium dodecyl sulfate–polyacrylamide gel electrophoresis (SDS–PAGE) and transferred to polyvinylidene difluoride membranes (BioRad Laboratories, CA). Immunoblotting was performed using anti-acetyl-H3, anti-acetyl-H4, anti-caspase 3, anti-caspase 4, anti-caspase 6, anti-caspase 7, anti-caspase 8, anti-caspase 9, anti-caspase 12, anti-poly(ADP-ribose) polymerase (PARP), anti-cIAP1, anti-cIAP2, anti-XIAP, anti-survivin, anti-livin, and anti-tubulin antibodies obtained from Cell Signaling Technology.

Analytical and statistical methods

The mean, standard deviation, Spearman correlation, and sign test were calculated using Microsoft's Excel software and R (R Foundation for Statistical Computing). A p -value of ≤ 0.05 was deemed to be significant.

Results

Effect of vorinostat alone and in combination with bortezomib on cytotoxicity of BCWM.1 cells

We previously reported that the expression level of HDACs (HDAC4, HDAC9, and Sirt5) in bone

marrow CD19+ cells isolated from patients with WM was significantly different from that of healthy donors [33]. We therefore sought to examine the effect of the prototypic HDAC inhibitor, vorinostat, on WM tumor cell killing using BCWM.1 cells. BCWM.1 cells were cultured with medium alone or vorinostat at escalating doses (0–5 μM) for 24 h prior to examination for apoptosis by annexin V–FITC and PI staining. We determined that the 50% inhibitory concentration (IC_{50}) for BCWM.1 cells was 4 μM (Figure 1). The IC_{50} for primary WM CD19+ cells ranged from 0.5 to 2 μM (Figure 2). BCWM.1 cells were next cultured with medium, vorinostat (0–5 μM) alone, and in combination with sublethal doses of bortezomib (0–45 pg/mL) for 24 h prior to annexin V and PI staining (Figure 1). The combinational effect of the drugs was determined using CalcuSyn [34] (Figure 1). Vorinostat and bortezomib resulted in synergistic increased cell killing over a wide range of tested doses in BCWM.1 cells. The optimal synergistic dose combination was determined to be 3 μM of vorinostat with 30 pg of bortezomib, which resulted in a mean apoptosis of $75.4 \pm 4.9\%$ at 24 h. We next performed a time course experiment using BCWM.1 cells treated with vorinostat (3 μM), bortezomib (30 pg), and both for 0, 6, 12, and 24 h. The percentage of apoptosis when BCWM.1 cells were treated with vorinostat (3 μM) was $2.37 \pm 0.96\%$, $2.54 \pm 0.68\%$, $2.15 \pm 0.42\%$, and $12.41 \pm 1.03\%$ at 0, 6, 12, and 24 h. The percentage of apoptosis when BCWM.1 cells were treated with bortezomib (30 pg) was $2.37 \pm 0.96\%$, $6.87 \pm 0.54\%$, $30.66 \pm 3.21\%$, and $57.01 \pm 1.31\%$ at 0, 6, 12, and 24 h. The percentage of apoptosis when BCWM.1 cells were treated with both vorinostat and bortezomib was $2.37 \pm 0.96\%$, $5.97 \pm 1.45\%$, $42.39 \pm 8.96\%$, and $73.81 \pm 2.36\%$ at 0, 6, 12, and 24 h, with a p -value of 0.035. The combined apoptotic effect of bortezomib and vorinostat did not increase proportionally to the dosing increase in either bortezomib or vorinostat. Therefore, sublethal doses of bortezomib and vorinostat were used in the subsequent experiment to decrease potential toxicity.

Effect of vorinostat alone and in combination with bortezomib on primary WM cell cytotoxicity

We next evaluated the effect of vorinostat, alone and in combination with bortezomib, on primary WM tumor cells. CD19+ bone marrow cells were isolated from nine previously treated patients with WM. These cells were then cultured with medium alone, sublethal doses of bortezomib (0–45 pg/mL), vorinostat (0.5–2 μM), or both for 24 h (Figure 2). Sublethal doses of bortezomib were used in this

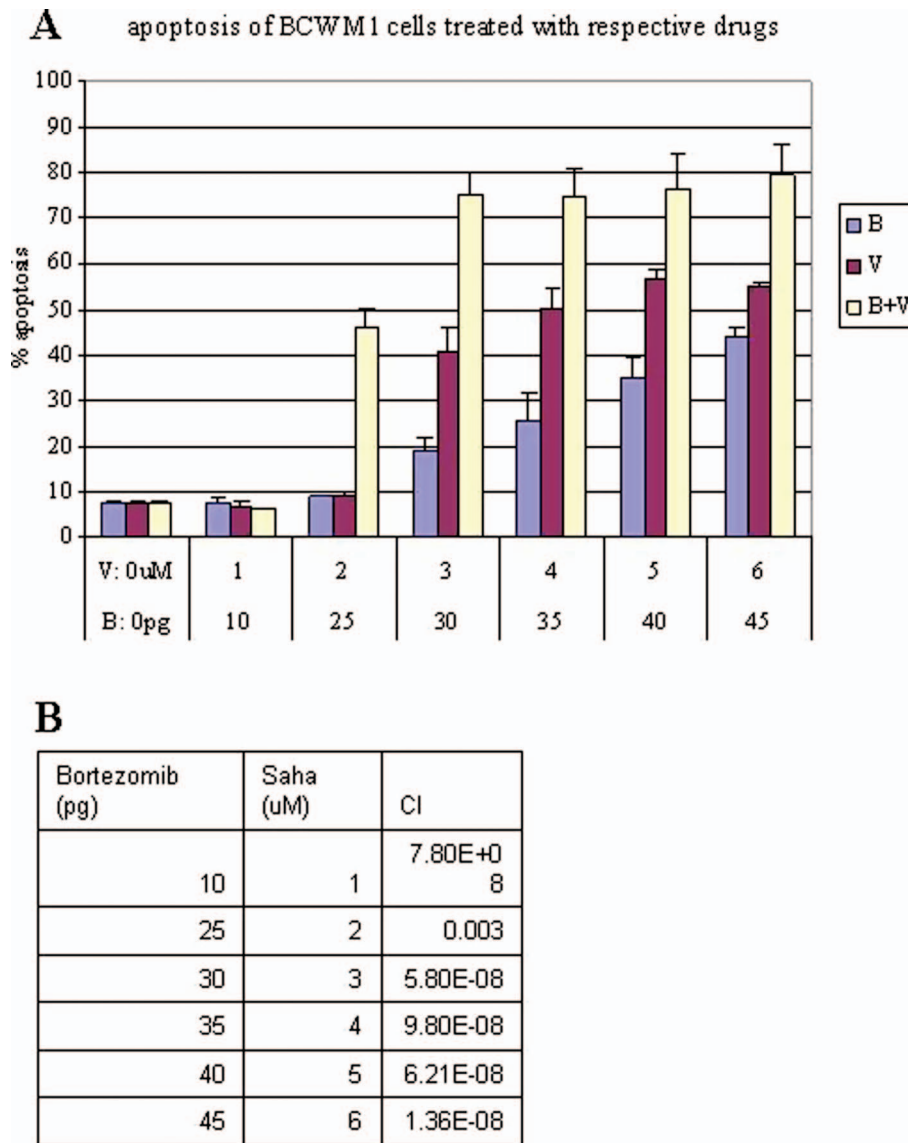


Figure 1. Cell killing effect of vorinostat as monotherapy and in combination with bortezomib in BCWM.1 WM cells. (A) BCWM.1 cells were cultured with vorinostat, V, alone and in combination with bortezomib, B, for 24 h prior to annexin V and PI staining. One of the three representative experiments is shown. (B) The combination indices (CI) of bortezomib and vorinostat are shown.

study due to its dose-dependent toxicity as shown by Orłowski *et al.* [35]. The dosing ranges determined from experiments with BCWM.1 cells were used in the treatment of primary WM cells, given the relative scarcity of primary WM cells. A mean change in apoptosis over untreated cells of 11.98%, 73.59%, and 84.39% was observed by annexin V and PI staining at 24 h when primary WM CD19+ cells were treated with bortezomib, vorinostat, or both, compared to medium alone. In contrast, a minimal change in apoptosis was observed when PBMC CD19+ cells were cultured with vorinostat, bortezomib, or both, compared to medium alone (Figure 2). At the dose range examined, vorinostat was more effective than bortezomib in inducing apoptosis.

The combination of vorinostat and bortezomib was also more effective than bortezomib alone, while the combination of vorinostat and bortezomib did not significantly differ from vorinostat alone in inducing apoptosis in primary WM tumor cells isolated from patients with WM (Figure 2).

Caspase 7 and PARP were activated much earlier than other caspases in vorinostat treated BCWM.1 cells

We next performed experiments to elucidate the molecular mechanisms by which vorinostat induced WM cell death. BCWM.1 cells were cultured in medium alone, or in the presence of a sublethal dose of vorinostat (3.5 μ M), bortezomib (30 pg/mL), or

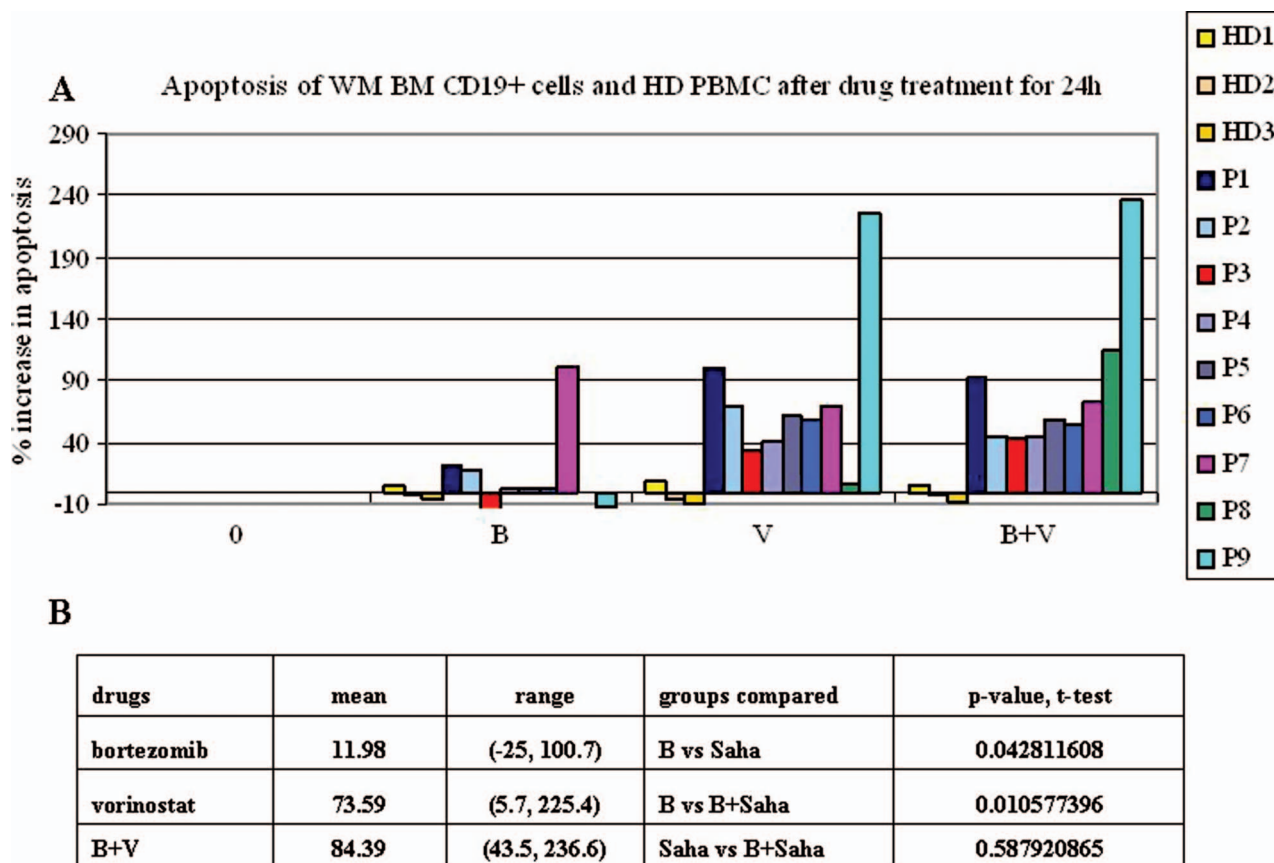


Figure 2. Apoptosis of WM bone marrow CD19+ cells and healthy donor PBMCs after treatment with bortezomib, B, vorinostat, V, or both. (A) CD19+ cells from three healthy donor PBMCs and nine WM bone marrow samples were isolated. CD19+ cells were cultured with medium, bortezomib, vorinostat, bortezomib plus vorinostat for 24 h prior to annexin V and PI staining. (B) Percentage change in apoptosis after drug treatment compared to control medium is shown.

vorinostat (3 μ M) plus bortezomib (30 pg/mL) for 0, 6, 12 and 24 h prior to cell lysate preparation and immunoblotting with anti-caspase 3, anti-caspase 4, anti-caspase 7, anti-caspase 8, anti-caspase 9, anti-caspase 12, anti-PARP, and anti-tubulin antibodies (Figure 3). There was basal activation of caspase 7 and PARP in untreated BCWM.1 cells. Increased cleavage of caspase 7 and PARP starting at 6 h were observed after treatment with vorinostat, compared to control. In contrast, caspase 3, caspase 6, and caspase 9 were not activated until 24 h following vorinostat treatment. In bortezomib treated BCWM.1 cells, there was a transient increase of cleaved caspases 3, 7, and 9 at 6 h, which returned to baseline at 12 h and did not reappear until 24 h. However, cleaved PARP did not appear until 24 h. When BCWM.1 cells were treated with vorinostat plus bortezomib, activation of caspases 3 and 7 and PARP peaked at 12 h and returned to baseline at 24 h. We also examined caspase 8 expression, although this was absent at baseline and following treatment (data not shown). There was no activation of caspase 6 in bortezomib or bortezomib plus

vorinostat treated BCWM.1 cells. The pattern of caspase activation was different in BCWM.1 cells treated with vorinostat alone, bortezomib alone, or bortezomib plus vorinostat. Most interesting, caspase 7 and PARP were activated much earlier than caspase 3 in vorinostat treated BCWM.1 cells.

Vorinostat down-regulated inhibitors of apoptosis in BCWM.1 cells

Since caspase 3 activation typically precedes that of caspase 7, the finding that caspase 7 was activated earlier than caspase 3 following vorinostat treatment of BCWM.1 cells suggested an alternative mechanism of activation for caspase 7. We therefore investigated IAPs as potential candidates for vorinostat related caspase 7 activation in WM. BCWM.1 cells were cultured with medium, vorinostat (3.5 μ M), bortezomib (30 pg/mL), or vorinostat (3 μ M) plus bortezomib (30 pg/mL) for 0, 6, 12 and 24 h prior to cell lysate preparation and immunoblotting with anti-cIAP1, anti-cIAP2, anti-XIAP, anti-survivin, anti-livin, and anti-tubulin antibodies

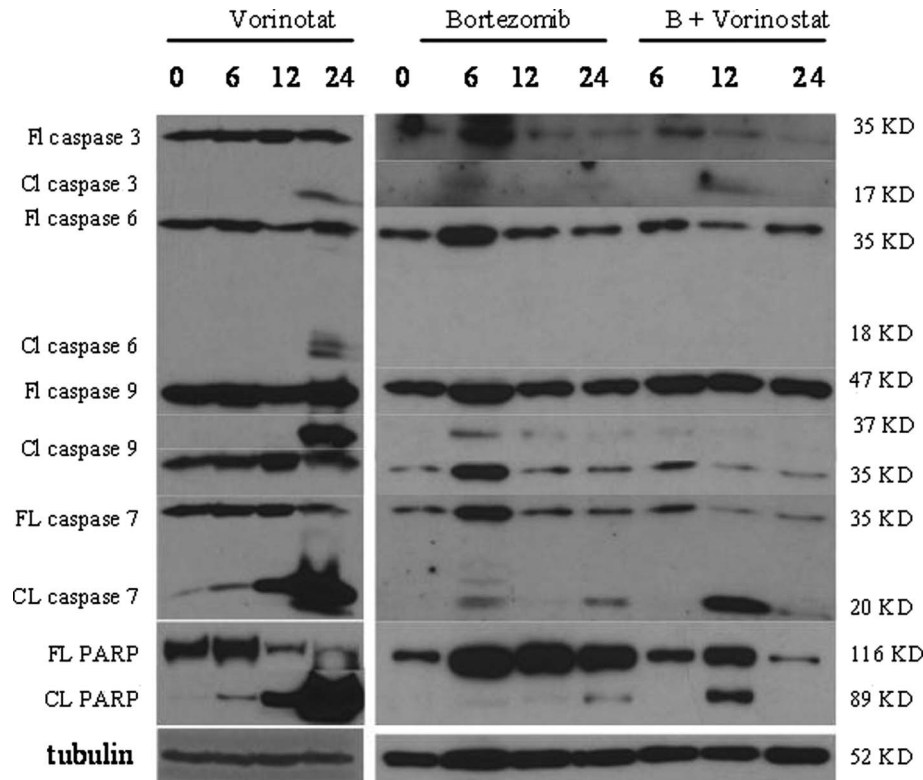


Figure 3. Western blot analysis for induction of apoptotic cascades, following treatment of BCWM.1 cells with bortezomib and vorinostat, alone and in combination. BCWM.1 WM cells were cultured with medium alone, bortezomib, vorinostat, or both for 0, 6, 12, and 24 h prior to immunoblotting. The major caspases and their activated counterparts are shown.

(Figure 4). In untreated BCWM.1 cells, cIAP1, cIAP2, XIAP, and survivin were expressed at high levels, though declined by 12 h following vorinostat treatment, and continuously declined by 24 h. XIAP was undetectable in BCWM.1 cells after 12 h of vorinostat treatment. The initial protein expression level of livin was lower compared to other IAPs tested here. There was a paradoxical increase in livin at 6 h after vorinostat treatment. However, the expression of livin protein was reduced after 24 h of vorinostat treatment compared to control (Figure 4).

Vorinostat inhibited HDAC activity in BCWM.1 cells

To demonstrate the direct inhibitory effect of vorinostat on HDACs, BCWM.1 cells were cultured with medium, vorinostat, bortezomib, or vorinostat plus bortezomib for 0, 6, 12, or 24 h prior to cell lysate preparation and immunoblotting with anti-acetyl-H3, anti-acetyl-H4, and anti-tubulin antibodies (Figure 5). Acetyl-H3 and acetyl-H4, which are substrates of HDACs, were increased following 6 h of vorinostat treatment in BCWM.1 cells. The levels of acetyl-H3 and acetyl-H4 were persistently elevated after 24 h treatment with vorinostat. In bortezomib treated BCWM.1 cells, acetyl-H3 and acetyl-H4 were increased after 6 h of treatment, but

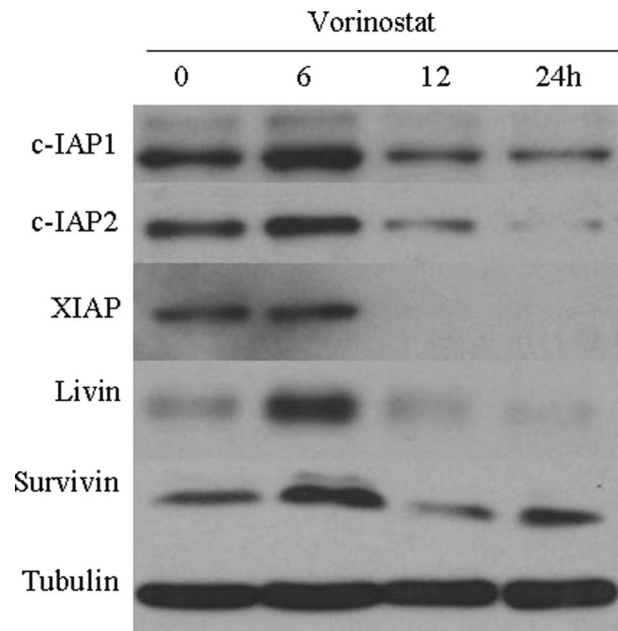


Figure 4. Effect of vorinostat on inhibitors of apoptosis (IAPs) in BCWM.1 WM cells. BCWM.1 cells were cultured with medium or vorinostat for 0, 6, 12, and 24 h prior to immunoblotting.

returned to baseline at 12 h. The level of acetyl-H3 and acetyl-H4 increased 6 h after treatment with bortezomib plus vorinostat, and remained elevated

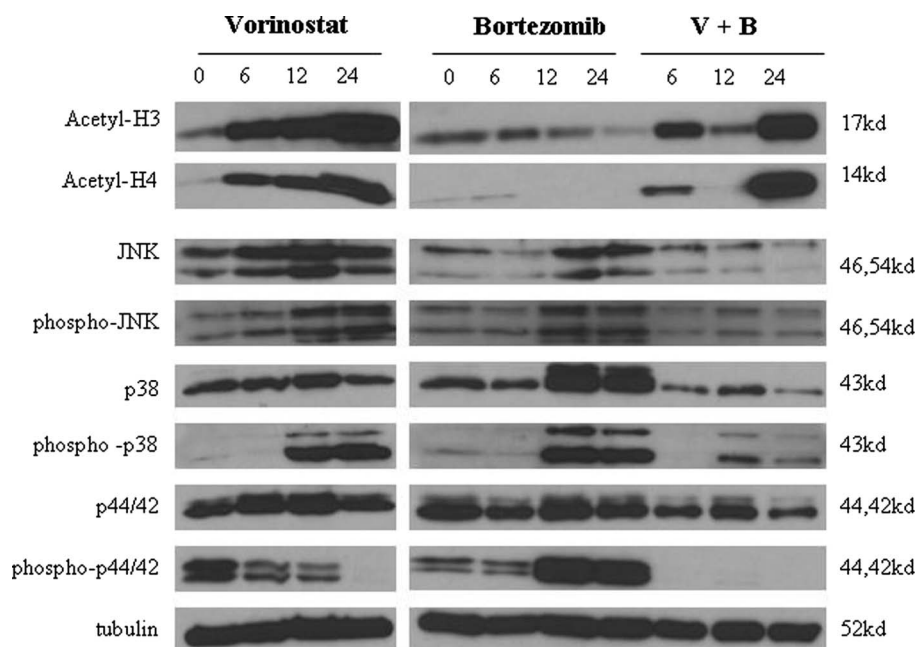


Figure 5. Effect of vorinostat and bortezomib, alone and in combination, on acetyl-H3, acetyl-H4, and MAPK pathways in BCWM.1 cells. BCWM.1 cells were cultured with medium, vorinostat, bortezomib, or both for 0, 6, 12, and 24 h prior to immunoblotting.

at 24 h. The increased acetyl-H3 and acetyl-H4 confirmed a decreased activity of HDACs after BCWM.1 cells were treated with vorinostat alone or in combination with bortezomib.

Vorinostat suppressed Erk pathway but activated p38 MAPK pathway

BCWM.1 cells were cultured with medium, vorinostat (3.5 μ M), bortezomib (30 pg/mL), or vorinostat (3 μ M) plus bortezomib (30 pg/mL) for 0, 6, 12, and 24 h prior to cell lysate preparation and immunoblotting with anti-Erk, anti-phospho-Erk, anti-p38 MAPK, anti-phospho-p38 MAPK, anti-JNK, anti-phospho-JNK, and anti-tubulin antibodies (Figure 5). The expression of Erk in BCWM.1 cells was increased after 6 h of vorinostat treatment and 12 h of bortezomib treatment, but decreased significantly when both drugs were combined. The activated Erk, phospho-Erk, was expressed at a high level in untreated cells, and reduced abruptly at 24 h following vorinostat treatment. Phospho-Erk in BCWM.1 was up-regulated 12 h following bortezomib treatment. There was no change in phospho-Erk expression when both bortezomib and vorinostat were combined. The level of p38 MAPK was unchanged when BCWM.1 cells were treated with vorinostat or bortezomib, but was decreased significantly with both drugs combined. There was a persistent increase in phospho-p38 MAPK after BCWM.1 cells were treated with vorinostat or bortezomib, starting at 12 h. The expression of phospho-p38 MAPK was

unchanged in vorinostat plus bortezomib treated BCWM.1 cells. JNK expression was elevated in vorinostat treated BCWM.1 cells, but was unchanged in bortezomib or vorinostat plus bortezomib treated cells. The expression of phospho-JNK was minimally detectable in vorinostat treated BCWM.1 cells and remained unchanged in BCWM.1 cells treated with bortezomib or bortezomib plus vorinostat.

Discussion

In this study, we sought to address the molecular pathways induced by vorinostat in WM cells. We observed by gene expression profiling (GEP) and quantitative real-time polymerase chain reaction (q-PCR) that HDAC expression in bone marrow lymphoplasmacytic cells was different between patients with WM and healthy donors. The HDAC expression pattern in BCWM.1 cells was more similar to that in WM CD19+ cells compared to healthy donor CD19+ cells [3]. Akin to our results with BCWM.1 WM cells, vorinostat also demonstrated significant apoptosis of primary WM cells, which occurred at micromolar ranges. In contrast, vorinostat did not produce significant apoptosis in healthy donor CD19+ cells. This difference may reflect the ability of vorinostat to alter the activity of HDACs, suggested by our findings of increased acetyl-H3 and acetyl-H4 expression following vorinostat treatment in BCWM.1 cells. The differential cytotoxicity may also reflect different baseline genomic stability between healthy donor CD19+ cells and

WM tumor cells, as tumor cells have higher genomic instability and a greater mutation rate.

We also observed that vorinostat had synergistic anti-tumor effects when combined with bortezomib in BCWM.1 cells over a wide range of dosing combinations. Vorinostat alone was more effective than bortezomib in inducing apoptosis in WM CD19+ cells. While the combination of vorinostat plus bortezomib showed accentuated WM tumor cell killing compared to bortezomib alone, this combination did not accentuate that observed with vorinostat alone. Others have reported that the extent of apoptosis can be impacted by the sequence of drug administration [36]. Experiments addressing the sequential administration of bortezomib followed by vorinostat (or vice versa) warrant further exploration. While others have demonstrated increased anti-tumor activity in combinations of HDAC inhibitors and bortezomib by preclinical studies using multiple myeloma and mantle cell lymphoma, these studies have predominantly relied on cell line data [29,36,37], which may not be reflective of primary tumor cells.

To address the mechanism of vorinostat induced-apoptosis in WM cells, we studied the activation of caspases, given their critical role in apoptosis [38]. We showed that vorinostat- and bortezomib-induced apoptosis in BCWM.1 cells was associated with activation of the mitochondrial dependent and ER stress-induced apoptosis pathways by activating caspase 3, caspase 6, caspase 7, and caspase 9. We also observed that caspase 7 and PARP were activated earlier, starting at 6 h, while caspases 3, 6, and 9 were activated 24 h after vorinostat treatment. We therefore hypothesized that the regulators of caspase 7 might be affected by vorinostat at an earlier time point. Further investigation confirmed that there was significant down-regulation of IAP family members, including c-IAP1, c-IAP2, XIAP, survivin, and livin after 12 h of treatment with vorinostat, which may allude to greater sensitivity for IAPs in modulating caspase 7 versus caspase 3 in WM cells. While c-IAP1 degradation was caspase 8 dependent in TRAIL (tumor necrosis factor-related apoptosis-inducing ligand)-induced apoptosis of liver cancer cells [39], IAP down-regulation was shown to be caspase-independent in human promyelocytic leukemia cells [40]. Further investigation of whether IAP down-regulation is caspase-dependent in WM would be interesting. The reduction in the IAPs could not solely be due to caspase-dependent degradation given that the tubulin level remained unchanged, and the degree of reduction in each of the IAPs varied.

The suppressive effect of vorinostat on IAPs could be through multiple mechanisms. Increased acetyl-H3 and acetyl-H4 after vorinostat treatment allows higher and dysregulated genomic transcription,

resulting in greater ER stress. The internal ribosome entry site elements present in cIAP1 and cIAP2 (cIAP1/2) abrogate their up-regulation during ER stress. A reduction in cIAP1/2 decreases the expression of XIAP, which is the most potent IAP to inhibit caspases 3, 7, and 9 [21]. ER stress suppresses cIAP1/2 directly and XIAP indirectly, resulting in decreased expression of cIAP1/2 and a dramatic decrease in XIAP. The reduction in these IAPs allows caspases 3, 7, and 9 to be activated. The reason for the paradoxical increase of livin in BCWM.1 cells at 6 h after vorinostat treatment is unclear at this point. The paradoxical increase in livin may reflect the initial response of BCWM.1 cells to vorinostat induced cellular stress by preferentially increasing the transcription and translation of livin, as is seen in the increase of XIAP, cIAP1, and cIAP2 in other tumor cells treated with vorinostat [18–20]. Our result is in accordance with the observation of others, and provides a mechanistic explanation as to how vorinostat induces apoptosis in WM cells through the activation of specific caspases. While Mitsiades *et al.* showed that there was a lack of involvement of caspases in vorinostat-induced apoptosis in multiple myeloma [41], this differential utilization of caspases is likely due to an intrinsic difference between multiple myeloma and Waldenstrom macroglobulinemia.

Cellular stress induced by vorinostat is also known to activate MAPK pathways, as observed in human T-cell lymphoma cells and Philadelphia chromosome bearing leukemic cells [42,43]. We further studied the stress pathways including Erk, JNK, and p38 MAPK in vorinostat treated WM cells. The combination of vorinostat and bortezomib did not lead to increased phosphorylation of JNK and p38 MAPK versus vorinostat or bortezomib alone, even though a clear synergistic apoptotic effect of vorinostat and bortezomib in BCWM.1 cells was observed. This discrepancy could be due to the ability of vorinostat to block bortezomib-mediated activation of Erk. The pivotal anti-apoptotic role of Erk activation found in our studies is consistent with that reported by others, namely that inhibition of Erk activation increases bortezomib lethality in malignant B cells [44]. The total protein of JNK, p38, and Erk was unchanged when cells were treated with vorinostat alone, increased when cells were treated with bortezomib, and decreased when cells were treated with both drugs. The reduction in total protein indicates that vorinostat could potentially restore proteasome degradation of total JNK, p38 MAPK, and Erk in cells treated with bortezomib, implying the potential of vorinostat to overcome bortezomib resistance in WM cells.

It is known that histone H3 phosphoacetylation is directly mediated by MSK1 (mitogen and stress activated kinase 1) via activation of MAPK pathways

[45,46]. As discussed earlier, acetylated H3 increases global transcription and ER stress and decreases IAP expression, which further augment caspase activation, with the resultant formation of an auto-amplification loop toward cell death. The caspase activation pattern was dramatically different in cells treated with vorinostat, bortezomib, or vorinostat plus bortezomib, which underscored the different mechanisms utilized by specific drugs prior to the common apoptotic pathway. In bortezomib treated BCWM.1 cells, the fluctuation of cleaved caspases 3, 7, and 9 is likely due to a survival signal from the activation of Erk pathways starting at 12 h. Even though the activated Erk signal persisted until 24 h, it is likely overcome by other altered signals from p38, NF- κ B, and AKT pathways, with the overall balance tipping toward final apoptosis, as shown in our and other studies [6,47].

To our knowledge, this is the first study to address the effect of vorinostat on the MAPK pathway in B-cell lymphoma and leukemia. The altered activation of Erk and p38 MAPK pathways is associated with a reduction in cIAP1, cIAP2, XIAP, and livin following the treatment of WM cells with vorinostat. Taken together, these studies support that stress induced apoptosis in WM cells is mediated through disrupting the balanced activity between the Erk and p38 MAPK pathways. Vorinostat induced cellular stress results in activation of the p38 MAPK pathway and a reduction of the IAP family members, leading to early activation of caspase 7. While the inhibition of the Erk pathway by vorinostat results in delayed activation of caspases 3, 6, and 9 at 24 h, the collective signaling strength of p38 MAPK activation as well as inhibition of Erk likely determines the apoptotic fate of WM cells upon vorinostat treatment.

In conclusion, vorinostat induced cellular stress disrupts the p38 MAPK and Erk pathways leading to apoptosis in WM cells. These studies provide further support of histone deacetylase inhibitors as therapeutic agents for the treatment of Waldenström macroglobulinemia.

Acknowledgements

This study is supported by the International Waldenström's Macroglobulinemia Foundation, the Bing Fund for Waldenström's Macroglobulinemia, the Bailey Family Fund for Waldenström's Research, and the Linda and Edward Nelson Fund for Waldenström's Macroglobulinemia.

Philip Brodsky provided graphical assistance.

Potential conflict of interest: Disclosure forms provided by the authors are available with the full text of this article at Disclosure.

References

1. Dimopoulos MA, Kyle RA, Anagnostopoulos A, et al. Diagnosis and management of Waldenström's macroglobulinemia. *J Clin Oncol* 2005;23:1564–1577.
2. Treon SP, Hatjiharissi E, Merlini G. Waldenström's macroglobulinemia/lymphoplasmacytic lymphoma. *Cancer Treat Res* 2008;142:211–242.
3. Hatjiharissi E, Mitsiades CS, Ciccarelli BT, et al. Comprehensive molecular characterization of malignant and microenvironmental cells in Waldenström's macroglobulinemia by gene expression profiling. *Blood* 2007;110(Suppl. 1): Abstract 3174.
4. Eot-Houllier G, Fulcrand G, Magnaghi-Jaulin L, et al. Histone deacetylase inhibitors and genomic instability. *Cancer Lett* 2009;274:169–176.
5. Johnstone RW. Histone-deacetylase inhibitors: novel drugs for the treatment of cancer. *Nat Rev Drug Discov* 2002;1:287–299.
6. Dai Y, Rahmani M, Dent P, et al. Blockade of histone deacetylase inhibitor-induced RelA/p65 acetylation and NF-kappaB activation potentiates apoptosis in leukemia cells through a process mediated by oxidative damage, XIAP downregulation, and c-Jun N-terminal kinase 1 activation. *Mol Cell Biol* 2005;25:5429–5444.
7. Finnin MS, Donigian JR, Cohen A, et al. Structures of a histone deacetylase homologue bound to the TSA and SAHA inhibitors. *Nature* 1999;401:188–193.
8. Marks PA, Richon VM, Rifkind RA. Histone deacetylase inhibitors: inducers of differentiation or apoptosis of transformed cells. *J Natl Cancer Inst* 2000;92:1210–1216.
9. Richon VM, Sandhoff TW, Rifkind RA, et al. Histone deacetylase inhibitor selectively induces p21WAF1 expression and gene-associated histone acetylation. *Proc Natl Acad Sci USA* 2000;97:10014–10019.
10. Ruefli AA, Ausserlechner MJ, Bernhard D, et al. The histone deacetylase inhibitor and chemotherapeutic agent suberoylanilide hydroxamic acid (SAHA) induces a cell-death pathway characterized by cleavage of Bid and production of reactive oxygen species. *Proc Natl Acad Sci USA* 2001;98:10833–10838.
11. Rosato RR, Grant S. Histone deacetylase inhibitors: insights into mechanisms of lethality. *Expert Opin Ther Targets* 2005;9:809–824.
12. Dokmanovic M, Marks PA. Prospects: histone deacetylase inhibitors. *J Cell Biochem* 2005;96:293–304.
13. Dubrez-Daloz L, Dupoux A, Cartier J. IAPs: more than just inhibitors of apoptosis proteins. *Cell Cycle* 2008;7:1036–1046.
14. Salvesen GS, Duckett CS. IAP proteins: blocking the road to death's door. *Nat Rev Mol Cell Biol* 2002;3:401–410.
15. Perrelet D, Ferri A, Liston P, et al. IAPs are essential for GDNF-mediated neuroprotective effects in injured motor neurons in vivo. *Nat Cell Biol* 2002;4:175–179.
16. Potts MB, Vaughn AE, McDonough H, et al. Reduced Apaf-1 levels in cardiomyocytes engage strict regulation of apoptosis by endogenous XIAP. *J Cell Biol* 2005;171:925–930.
17. Conte D, Holcik M, Lefebvre CA, et al. Inhibitor of apoptosis protein cIAP2 is essential for lipopolysaccharide-induced macrophage survival. *Mol Cell Biol* 2006;26:699–708.
18. Warnakulasuriarachchi D, Cerquozzi S, Cheung HH, et al. Translational induction of the inhibitor of apoptosis protein HIAP2 during endoplasmic reticulum stress attenuates cell death and is mediated via an inducible internal ribosome entry site element. *J Biol Chem* 2004;279:17148–17157.
19. Lewis SM, Holcik M. IRES in distress: translational regulation of the inhibitor of apoptosis proteins XIAP and HIAP2 during cell stress. *Cell Death Differ* 2005;12:547–553.

20. Warnakulasuriyarachchi D, Ungureanu NH, Holcik M. The translation of an antiapoptotic protein HIAP2 is regulated by an upstream open reading frame. *Cell Death Differ* 2003; 10:899–904.
21. Hamanaka RB, Bobrovnikova-Marjon E, Ji X, et al. PERK-dependent regulation of IAP translation during ER stress. *Oncogene* 2009;28:910–920.
22. Zweifach A, Lewis SA. Characterization of a partially degraded Na⁺ channel from urinary tract epithelium. *J Membr Biol* 1988;101:49–56.
23. Hunter T. Oncoprotein networks. *Cell* 1997;88:333–346.
24. Milella M, Kornblau SM, Estrov Z, et al. Therapeutic targeting of the MEK/MAPK signal transduction module in acute myeloid leukemia. *J Clin Invest* 2001;108:851–859.
25. Lee ER, McCool KW, Murdoch FE, et al. Dynamic changes in histone H3 phosphoacetylation during early embryonic stem cell differentiation are directly mediated by mitogen- and stress-activated protein kinase 1 via activation of MAPK pathways. *J Biol Chem* 2006;281:21162–21172.
26. Lane SW, Scadden DT, Gilliland DG. The leukemic stem cell niche: current concepts and therapeutic opportunities. *Blood* 2009;114:1150–1157.
27. Chen CI, Kouroukis CT, White D, et al. Bortezomib is active in patients with untreated or relapsed Waldenstrom's macroglobulinemia: a phase II study of the National Cancer Institute of Canada Clinical Trials Group. *J Clin Oncol* 2007;25:1570–1575.
28. Dimopoulos MA, Gertz MA, Kastritis E, et al. Update on treatment recommendations from the Fourth International Workshop on Waldenstrom's Macroglobulinemia. *J Clin Oncol* 2009;27:120–126.
29. Heider U, vonMetzler I, Kaiser M, et al. Synergistic interaction of the histone deacetylase inhibitor SAHA with the proteasome inhibitor bortezomib in mantle cell lymphoma. *Eur J Haematol* 2008;80:133–142.
30. Mitsiades CS, Hayden PJ, Anderson KC, et al. From the bench to the bedside: emerging new treatments in multiple myeloma. *Best Pract Res Clin Haematol* 2007;20:797–816.
31. Richardson P, Mitsiades C, Schlossman R, et al. The treatment of relapsed and refractory multiple myeloma. *Hematology Am Soc Hematol Educ Program* 2007:317–323.
32. DitzelSantos D, Ho AW, Tournilhac O, et al. Establishment of BCWM.1 cell line for Waldenstrom's macroglobulinemia with productive in vivo engraftment in SCID-hu mice. *Exp Hematol* 2007;35:1366–1375.
33. Sun JY, Xu L, Tseng H, et al. Histone deacetylase inhibitors demonstrate significant preclinical activity as single agents, and in combination with bortezomib in Waldenstrom's macroglobulinemia. *Clin Lymphoma Myeloma Leuk* 2011;11:152–156.
34. Chou TC. Theoretical basis, experimental design, and computerized simulation of synergism and antagonism in drug combination studies. *Pharmacol Rev* 2006;58:621–681.
35. Orłowski RZ, Stinchcombe TE, Mitchell BS, et al. Phase I trial of the proteasome inhibitor PS-341 in patients with refractory hematologic malignancies. *J Clin Oncol* 2002;20:4420–4427.
36. Pei XY, Dai Y, Grant S. Synergistic induction of oxidative injury and apoptosis in human multiple myeloma cells by the proteasome inhibitor bortezomib and histone deacetylase inhibitors. *Clin Cancer Res* 2004;10:3839–3852.
37. Catley L, Weisberg E, Kiziltepe T, et al. Aggrosome induction by proteasome inhibitor bortezomib and alpha-tubulin hyperacetylation by tubulin deacetylase (TDAC) inhibitor LBH589 are synergistic in myeloma cells. *Blood* 2006;108:3441–3449.
38. Yuan J, Horvitz HR. A first insight into the molecular mechanisms of apoptosis. *Cell* 2004;116:S53–S56, 1 p following S59.
39. Guicciardi ME, Mott JL, Bronk SF, et al. Cellular inhibitor of apoptosis 1 (cIAP-1) degradation by caspase 8 during TNF-related apoptosis-inducing ligand (TRAIL)-induced apoptosis. *Exp Cell Res* 2011;317:107–116.
40. Doyle BT, O'Neill AJ, Newsholme P, et al. The loss of IAP expression during HL-60 cell differentiation is caspase-independent. *J Leukoc Biol* 2002;71:247–254.
41. Mitsiades N, Mitsiades CS, Richardson PG, et al. Molecular sequelae of histone deacetylase inhibition in human malignant B cells. *Blood* 2003;101:4055–4062.
42. Yu C, Rahmani M, Conrad D, et al. The proteasome inhibitor bortezomib interacts synergistically with histone deacetylase inhibitors to induce apoptosis in Bcr/Abl⁺ cells sensitive and resistant to STI571. *Blood* 2003;102:3765–3774.
43. Zhang QL, Wang L, Zhang YW, et al. The proteasome inhibitor bortezomib interacts synergistically with the histone deacetylase inhibitor suberoylanilide hydroxamic acid to induce T-leukemia/lymphoma cells apoptosis. *Leukemia* 2009;23:1507–1514.
44. Orłowski RZ, Small GW, Shi YY. Evidence that inhibition of p44/42 mitogen-activated protein kinase signaling is a factor in proteasome inhibitor-mediated apoptosis. *J Biol Chem* 2002; 277:27864–27871.
45. Lin H, Chen C, Li X, et al. Activation of the MEK/MAPK pathway is involved in bryostatin1-induced monocytic differentiation and up-regulation of X-linked inhibitor of apoptosis protein. *Exp Cell Res* 2002;272:192–198.
46. Vrana JA, Grant S. Synergistic induction of apoptosis in human leukemia cells (U937) exposed to bryostatin 1 and the proteasome inhibitor lactacystin involves dysregulation of the PKC/MAPK cascade. *Blood* 2001;97:2105–2114.
47. Leleu X, Jia X, Runnels J, et al. The Akt pathway regulates survival and homing in Waldenstrom macroglobulinemia. *Blood* 2007;110:4417–4426.